

Three Dimensional Bulk Index Inhomogeneity Measurement using Computed Tomography

B. L. Stamper, J. H. Burge, W. J. Dallas

Optical Sciences Center/University of Arizona, Tucson, AZ 85721

ABSTRACT

Manufacturers of optical glass strive to make a product that is homogeneous, isotropic, and free of any bubbles or mechanical strain. Glass used in forming images is very good, but the process of mixing the constituent materials, and melting them into a glass is limited. As uniform as the mixtures are, they are not perfect, and the effects can be seen anytime light must propagate through several centimeters of glass. One method for measuring the three dimensional inhomogeneities in a piece of glass will be shown. Interferometry and computed tomography will be used to map the bulk refractive index variations. Having three dimensional information on the refractive index is the first step in compensating for errors in an imaging system.

Keywords: refractive index, inhomogeneity, computed tomography

1. INTRODUCTION

Homogeneity is the most important requirement for glass intended to form images.¹ Refractive index inhomogeneities are inherent errors remaining from the manufacturing process. Even though a great deal of effort is exerted to making very homogeneous, isotropic optical glasses, this perfection is never quite achieved.² Mixing mechanics is the dominate process for this phenomenon as several materials come together simultaneously. The result is a variation of index with position. A purely homogeneous piece of glass will allow light to propagate without any change in direction as it traverses the glass. Small changes in index will bend the light during its journey through the glass, culminating in degradation of the final image.

Currently, interferometry is used to analyze the refractive index variations in which measurements are integrated along the test beam. Any changes along the optical axis are averaged along the length of the glass piece. It is common to use index matching fluid and polished windows of known surface figure to reduce the error during refraction of the test beam into the sample. Inhomogeneity is then specified using a single number - the peak to valley change found within the glass sample. Not only have we lost the longitudinal information, data about the texture of the two transverse axes is also gone. An inclusion may have a small volume, but will be shown to extend the length of the sample along the test axis. The magnitude of the index change caused by the inclusion has been averaged with the other values along the test axis.

Using computed tomography will allow information along the test axis to be restored so the magnitude and location of index changes can be determined. The same interferometric technique will be used to gather the necessary test data for a glass sample. However, many more measurements are to be taken as the glass is rotated. The set of optical path data will be used to build a three dimensional array that corresponds to the refractive index at any point in the bulk sample of glass.

Further author information: (Send correspondence to BS)

BS: stamper@optics.arizona.edu

JB: jburge@optics.arizona.edu

WD: dallas@radiology.arizona.edu

2. COMPUTED TOMOGRAPHY

Tomography techniques involve reconstructing a picture of the object by measuring the transmission of the object. Data is taken with the sample rotated through many different, but known, angles. The most common method today is known as Computed Tomography (CT). More accurately, it is called computed trans-axial tomography. In medical imaging where people are the objects of importance, the source is commonly x-rays or gamma rays. The reconstructed plane is parallel to the beam of rays, and images are made one slice at a time.

In its simplest form, line integrals are taken for all straight lines through the region of measurement.^{3,4} Medical applications of tomography measure the density of an object based on absorption information while we want to measure small changes in optical path.⁵

2.1. Two Dimensional CT

We will describe the two dimensional procedure for ease of understanding. To expand to three dimensions only requires taking several two dimensional measurements at once. They are just stacked one on top of the other to build up the third dimension of our projection array.

The test beam, from a collimated source, goes through a plane of the sample. The irradiance detected exiting the sample is one projection as shown in Figure 1.

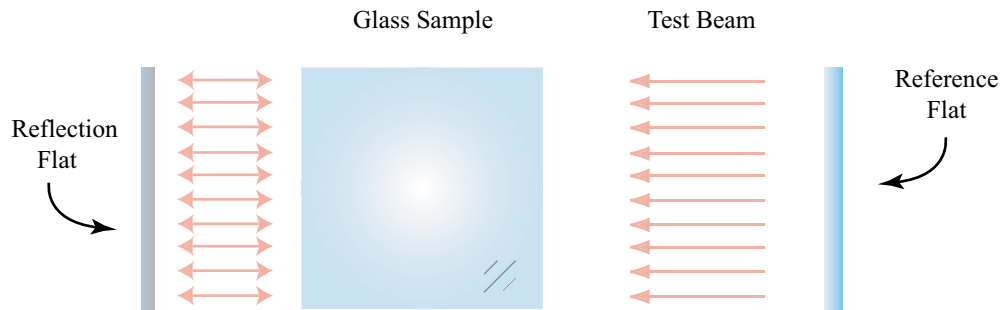


Figure 1. Geometry for making a single measurement, or projection.

We then build up an array of projections, each at a different angle as shown in Figure 2.

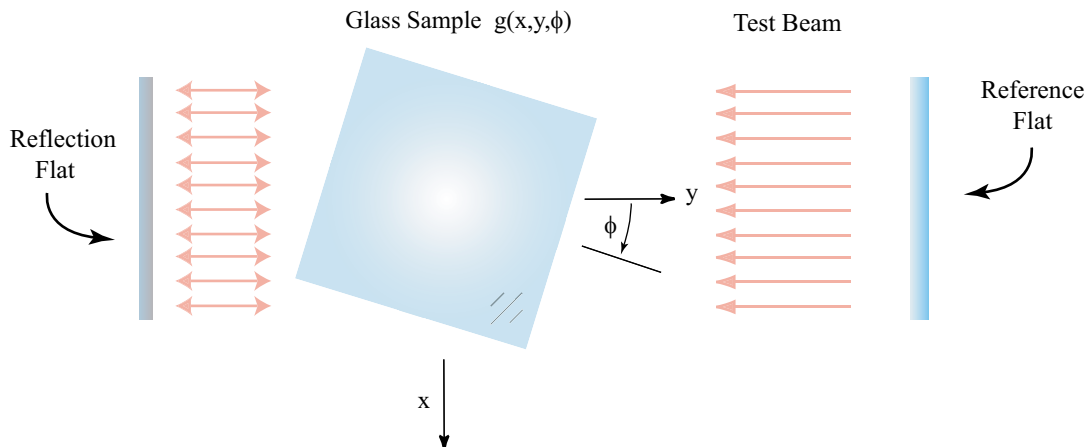


Figure 2. Rotation of sample between projections as needed for computed tomography.

This can be represented by Equation 1 as a summation through the sample:

$$p(x, \phi) = \int_{-\infty}^{\infty} w(y)g(x, y, \phi)dy. \quad (1)$$

Where $w(y)$ is a windowing function dictated by the extent of the measuring system. Each projection in our array will correspond to a specific angle of rotation. We then perform a one dimensional Fourier transform row by row shown in Equation 2:

$$p(\xi, \phi) = \int_{-\infty}^{\infty} \int_{-\infty}^{\infty} g(x, y, \phi)e^{-2\pi(\xi x + 0y)}dxdy = G(\xi, 0, \phi). \quad (2)$$

A new two dimensional array is built by taking each row of our transformed array, and placing it at the proper angle in a blank array. Each row is placed on top of the previous row, but at its corresponding angle illustrated in Figure 3. This new array, $G(\xi, \eta)$, is the two dimensional Fourier transform of our object, but some data points are zero since we don't have samples at an infinite number of angles. We must fill in the rest of these points in the array.

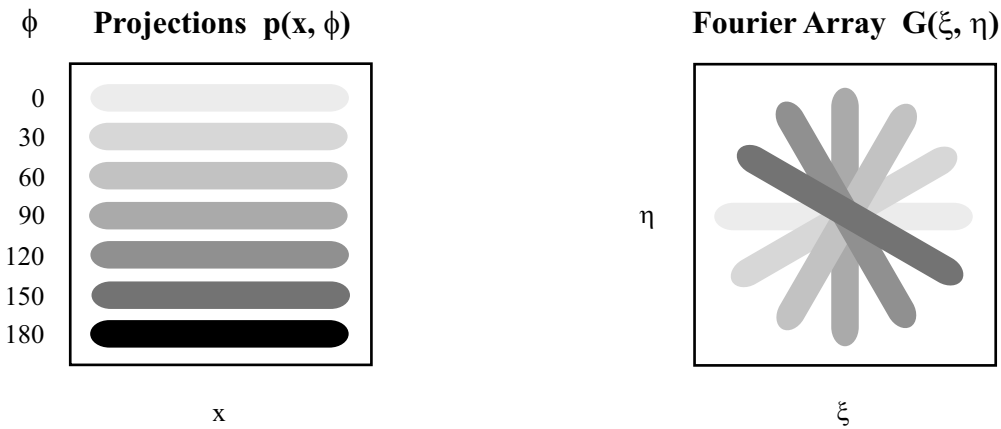


Figure 3. At left is a projection array made from individual measurements. At right is the resulting Fourier array after transforming each row of the projection array, and placing into a blank array based on their corresponding angle. All blank locations will be filled in with the nearest non-zero value.

A simple way to fill blank values is to step through the Fourier array. Every time a blank is found, just fill it with the value to the left in the same row. This works, but causes a noisy reconstruction. A slight improvement is to find the nearest value in the same row. Better to find the absolute closest non-zero value, such as with a nearest neighbor sampling, regardless of its direction from the blank location.

Both steps can be done at once using a true nearest neighbor approach working from the Fourier array back to the projection information. Step through each location in the Fourier array, calculate the distance from the center, ρ , and the associated angle, ϕ . Find the nearest ϕ value in the projection array, then find the ξ value of that projection closest to ρ , and place that value in the Fourier Array. Keep in mind that here, ρ can be negative. This stems from the fact that only rotation through 180° is used to completely fill the two dimensional transform space. Only stepping through the bottom half of the 2D array is necessary. Since we have a projection value for this point, and its complimentary point directly across the center, why not fill both points now. So for every point we step through, we fill it, and its complimentary point resulting in $G(\xi, \eta)$ as in Figure 4. Perform the 2D inverse Fourier Transform on the final array to reconstruct the object.

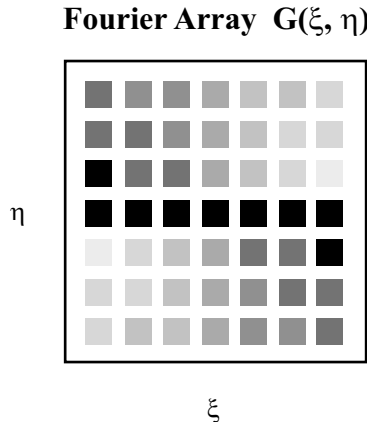


Figure 4. The Fourier array resulting when a nearest neighbor approach is used to fill each location.

The two methods differ in the direction that you fill the Fourier array. The first works from the projection array. Each projection is placed, adding the values that overlap, ρ filtering, then inverse transforming. We choose to work in the opposite direction by starting at the blank Fourier array. We then find the best value from the projections for each location. Then inverse transform to get the reconstructed object.

2.2. Filtering

When the next projection in sequence is written to the Fourier array, it may overlap locations that already have non-zero values from a previous projection. The simplest approach is to overwrite the value each time a new projection overlaps a previously written location. This works very well, and if coupled with a nearest neighbor method, is almost the same as our current method. A small improvement in accuracy, and complexity, adds the values that overlap. As new projections are added into the Fourier array, the central location becomes a large value. A ρ filter is used to adjust the values back to the correct order of magnitude.^{6,7} We simply multiply each value by its distance from the center.

Another method is to fill the Fourier array by interpolation. This is the same as a backprojection⁸ in direct space. Backprojection is a smearing of the y direction of the projections. Add the backprojections into the 2D direct space array. Transform this 2D array, ρ filter it, then inverse transform to reconstruct the object. This filtered backprojection improves upon the nearest neighbor approach, but is more difficult to implement, and requires some element of trial and error to determine how much to smear the projections.

3. SIMULATED THREE DIMENSIONAL OBJECT

Now that we have chosen a starting algorithm, we would like to chose an object that allows us to test the procedure. A simple cube in our larger 3D dataset shown on the left in Figure 5. The small internal object is a different refractive index than the surrounding material. Using a small internal object like this allows us to make sure our projections are correct. For a 2D slice through the cube, our projection array should produce a sinogram. The curve in the projection array is a function of the rotation angle, and this function is equivalent to a sine curve. As the sample is rotated, the sinusoidal curve traced by the feature is shown on the right in Figure 5.



Figure 5. A sample with a small object of a different refractive index. On the right is the associated sinogram projection matrix created as the internal feature is rotated. As shown, rotation is about the axis perpendicular to the plane of the object.

3.1. Limited Angle

In medical tomography there are no refractive properties of the subject to complicate the measurement. Using visible light, and a sample that is not circularly symmetric, will not allow 360° of rotation. A subset of measurements must be used as shown in Figure 6 for our square geometry. This is known as the limited angle problem, and can reduce the amount of information available to make an accurate reconstruction. The decrease in information that directly transfers to the Fourier array is not as disastrous for our object geometry as one might assume.⁹ Many other sample types don't give good results with this error. An example of how the reconstruction degrades is shown in Figure 7.

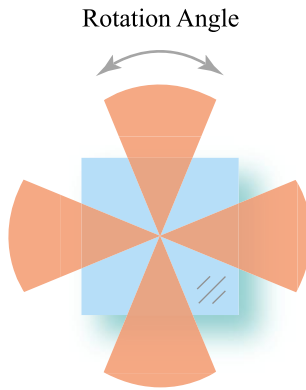


Figure 6. A sample with a limited range of angles available over which a projection can be made. The cones represent angles over which we can make measurements.

3.2. Region of Interest

When the available measurement aperture available is smaller than the extent of the sample, only a portion can be measured.^{10, 11} The test setup can often be changed to avoid this problem, but in the spirit of using instrumentation that is at hand, we would expect to see region of interest errors. Figure 8 shows how a reconstruction can degrade. A small feature in the sample can rotate into the measurement beam, and back out of it so that only a fraction of the projections have measured the feature in question. This can be compounded further as a limited angle is probably required if a region of interest problem is present.

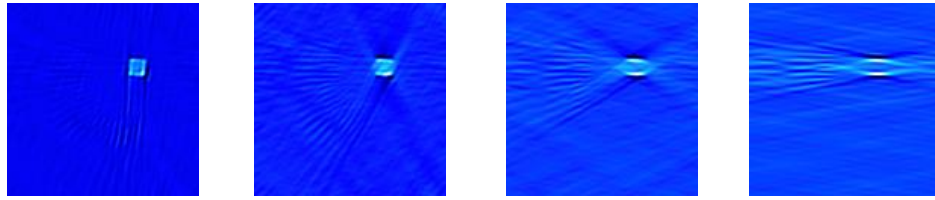


Figure 7. Degradation when limiting the measurement angle. From left to right we have a total view angle of 180° , 120° , 60° , 20° .

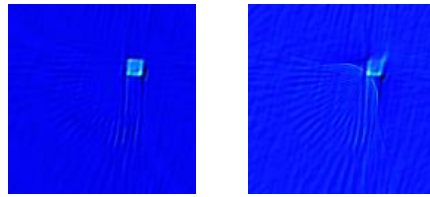


Figure 8. Effect of limiting the measurement aperture. The left is a full reconstruction while the right image has a region of interest imposed on the measurement.

3.3. Reconstruction Contrast

Applications where the density is measured prefer only that the aperture in question be bigger than the sample. Using an interferometer such as a laser fizeau that is double pass can introduce unwanted information in the measurement. When the aperture is bigger than the sample, the portion of the beam that doesn't intersect the sample is reflected by the reference flat and becomes part of the measurement. The optical path contributed by the flat must be removed from the measurement.

Simulations so far have used a background of zero, and an internal feature of magnitude equal to one. Object contrast is then equal to one, and we get the reconstruction as before. If we change the contrast of the object to $\frac{1}{2}$, or $\frac{1}{5}$, then the feature of interest starts to fade into the background of the reconstruction as shown in Figure 9. This decrease in contrast of the reconstruction is the subject of current work. It involves simply removing the contributions to the optical path not made by the sample of interest.

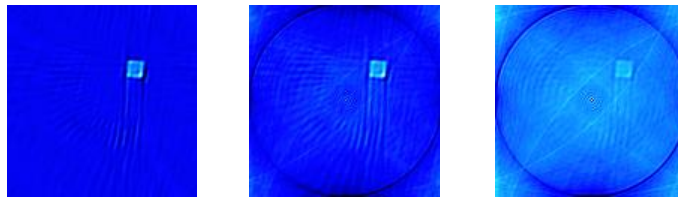


Figure 9. Our reconstruction for an object contrast equal to one is on the left. In the center we see the effect of decreasing the object contrast to $\frac{1}{2}$, and on the right of decreasing to $\frac{1}{5}$.

4. EXPERIMENTAL RESULTS

Hardware used to rotate the samples was made up of two motorized rotation stages on a custom angle bracket. Rotation can be in azimuth or elevation with the limit being determined by geometry of the sample or interference from the mounting bracket as it swings into the measurement beam during rotation. If azimuth only was used, a

full 360° would be possible, but the sample may limit the useful projection angles. Two glass samples are shown in Figure 10.



Figure 10. A cube glass sample at left, and a thin glass plate shown at right.

A WYKO 6000 laser fizeau was used to take the interferograms at 632.8nm . The interferometer will phase shift the allowing the proprietary software to produce a surface map based on the optical path through the sample. The downside is that noise can be introduced into the optical path data that it calculates, but this can be improved by averaging multiple measurements together. Each surface map is corrected for the .83 aspect ratio of the WYKO's detector and changed from 256×240 pixels on the detector to 256×256 used in our algorithm. The maps are then written into our projection array before being processed by our tomography routine.

The recent data taken on the glass cube and plate samples seems to have a large amount of structure unrelated to the sample. Figure 11 shows planes from their respective reconstructions. Diagonal striae present doesn't correspond to the surfaces of the glass. Features that should be readily apparent, such as the edges of the thin plate, aren't discernible in the reconstruction.

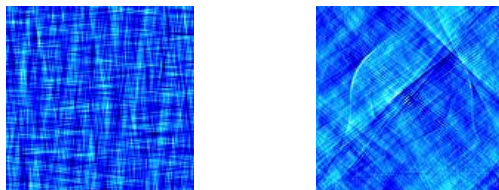


Figure 11. A slice perpendicular to the rotation axis at its midpoint from the 3D reconstruction for the cube glass sample is on the left. The slice shown at right also perpendicular to the rotation axis a quarter of the way from the top and is from a thin glass plate.

Comparing the simulations to the data shown above leads us to look closer at the contrast of our optical path measurements. The background information outside the sample that is entering the data dramatically reduces the contrast ratio of the reconstruction. Reconstructing the object is more sensitive to this error than expected. The next course of action is to determine the best way for subtracting the portion of the surface map produced by the background data. Taking an additional measurement without the sample in the test beam for each interferogram, then subtracting it from the sample test is the most straightforward approach. Finding the surface from the optical path map may work as well, and wouldn't require twice as many pieces of data. Looking closely at this problem is the next step in improving this technique.

5. CONCLUSION

The initial phase of an effort to improve optical glass inhomogeneity testing has been discussed. Using available interferometric techniques is a primary goal of this research. Eliminating the need to use index matching, whether

to attach windows to a sample or as a bath,¹² is another important goal. Use of common equipment and a simple algorithm would make inhomogeneity measurements more accessible. It would allow a specific piece of glass to be analyzed to insure internal features aren't incompatible with the final use of the glass. This could save many hours of labor grinding and polishing surfaces on a lens from glass that will not meet the intended goal.

Tomographic reconstruction has the advantage of recreating information along the measurement axis that is lost during single measurement techniques. A simple direct Fourier method of reconstruction has been presented. Many different methods of reconstructing an image using tomographic techniques are available,^{13, 14} and may be applied as our analysis of current errors progresses.

Simulation currently corresponds very well to problems encountered in actual data. Used in conjunction with experimental data, it has helped diagnose problems. Additional work will examine how well the optical surfaces involved in the test are recovered such as the reference surface, first sample surface, sample thickness, rear sample surface, and the reflection flat used. Continuing work will focus on removing background information being added to individual optical path measurements. An improvement in surface mapping will be investigated including refinements of our data processing algorithms.

ACKNOWLEDGMENTS

We are also glad to have had the help of Martin Valente and the optics shop at the Optical Science Center. This work is supported by NASA's Graduate Student Researchers Program, and in part by the University of Arizona's Small Grant in Imaging Science.

REFERENCES

1. T. S. Izumitani, *Optical Glass*, American Institute of Physics, 1986.
2. D. R. Uhlmann and N. J. Kreidl, eds., *Glass: Science and Technology*, vol. 2, Academic Press, 1984.
3. A. M. Cormack, "Representation of a function by its line integrals, with some radiological applications," *Journal of Applied Physics* **34**, pp. 2722–2727, 1963.
4. G. N. Hounsfield, "Computerized transverse axial scanning (tomography): Part I description of system," *British Journal of Radiology* **46**, pp. 1016–1022, 1973.
5. S. Cha and C. M. Vest, "Tomographic reconstruction of strongly refracting fields and its application to interferometric measurement of boundary layers," *Applied Optics* **20**, pp. 2787–2794, 1981.
6. H. H. Barrett and W. Swindell, *Radiological Imaging*, Academic Press, 1981.
7. R. N. Bracewell, *Two-Dimensional Imaging*, Prentice Hall, 1995.
8. R. N. Bracewell and A. C. Riddle, "Inversion of fan-beam scans in radio astronomy," *The Astrophysical Journal* **150**, pp. 427–434, 1967.
9. M. Y. Chiu, H. H. Barrett, R. G. Simpson, C. Chou, J. W. Arendt, and G. R. Gindi, "Three-dimensional radiographic imaging with a restricted view angle," *JOSA* **69**, pp. 1323–1333, 1979.
10. R. M. Lewitt, "Processing of incomplete measurement data in computed tomography," *Medical Physics* **6**, pp. 412–417, 1979.
11. R. N. Bracewell and S. J. Wernecke, "Image reconstruction over a finite field of view," *JOSA* **65**, pp. 1342–1346, 1975.
12. H. Suhara, "Interferometric measurement of the refractive-index distribution in plastic lenses by use of computed tomography," *Applied Optics* **41**, pp. 5317–5325, 2002.
13. D. W. Sweeney and C. M. Vest, "Reconstruction of three-dimensional refractive index fields from multidirectional interferometric data," *Applied Optics* **12**, pp. 2649–2664, 1973.
14. D. Verhoeven, "Limited-data computed tomography algorithms for the physical sciences," *Applied Optics* **32**, pp. 3736–3754, 1993.